Response of coal rock apparent resistivity to hydraulic fracturing process

Dazhao Song[1], Enyuan Wang[2,3], Liming Qiu[*2,3], Haishan Jia[2,3], Peng Chen[4] and Menghan Wei[1]

[1]*School of Civil and Resource Engineering, University of Science and Technology Beijing, Beijing 100083, China*
[2]*Key Laboratory of Gas and Fire Control for Coal Mines, China University of Mining and Technology, Xuzhou 221116, China*
[3]*School of Safety Engineering, China University of Mining and Technology, Xuzhou 221116, China*
[4]*Safety Engineering College of NCIST & Center, North China Institute of Science and Technology, Yanjiao 065201, China*

Abstract. In order to explore the comprehensive evaluation means of the extent of hydraulic fracturing region in coal seams, we analyzed the feasibility of detecting the response of coal rock direct current (DC) apparent resistivity to hydraulic-fracturing using Archie's theory, and conducted experimental researches on the response of DC resistivity in the hydraulic fracturing process using small-scale coal rock samples. The results show that porosity and water saturation are the two factors affecting the apparent resistivity of coal rock while hydraulic fracturing. Water has a dominant effect on the apparent resistivity of coal rock samples. The apparent resistivity in the area where water flows through is reduced more than 50%, which can be considered as a core affect region of hydraulic fracturing. Stress indirectly impacts the apparent resistivity by changing porosity. Before hydraulic fracturing, the greater axial load applied, the more serious the rupture in the samples, resulting in the greater apparent resistivity. Apparent resistivity testing is a potential regional method to evaluate the influence range of hydraulic fracturing in coal seams.

Keywords: coal rock mass; hydraulic fracturing; DC resistivity response; apparent resistivity

1. Introduction

In recent years, China's coal mines have introduced the hydraulic fracturing technique in oil and gas industry into coal mining for pressure relief and permeability improvement of difficult drainage coal seams. Experimental investigations (Huang *et al.* 2014, Lei and Wu 2014, Hou *et al.* 2013), numerical simulations (Yan *et al.* 2013, Zhou *et al.* 2013, Zhang *et al.* 2014) and field measurements (Li *et al.* 2013, Zhu *et al.* 2014, Ashoori *et al.* 2015) all have proven that hydraulic fracturing can effectively relieve gas pressure, increase gas permeability into coal seams, greatly improve gas drainage efficiency, and ultimately achieve both good gas drainage and outburst prevention.

The most key step in hydraulic fracturing technique applications is determination of the fractured zone. If it is determined reasonably, the engineering workload of gas drainage at the late stage at the mining site will be greatly reduced under without sacrificing the safe production of coal mining. Otherwise, the stress may inhomogeneously distributed on both sides of the single fractured crack or among the fractured cracks after coal rock fracturing, forming the stress concentration zone in the coal seams, evening inducing coal and gas outbursts. At present, the disturbance range of hydraulic fracturing is still determined using very traditional means, such as measuring the amount of drill cuttings, water content, gas drainage effect, etc.

(Chen 2012, Lin 2010). However, these parameters are only "point evaluation" of the potential regions impacted by hydraulic fracturing. In other words, these parameters are measured by extracting coal cores at fixed positions within the possible regions to assess whether hydraulic fracturing could affect the positions. Obviously, the method is no way to realize a comprehensive, continuous, spatiotemporal assessment of the coal rock structure within the regions. Thus, to some extent, it makes the late gas drainage construction blind, not only affecting the production safety but also greatly increasing the construction costs.

In recent years, many geoelectric techniques have been widely applied to the coal mine prospecting field (Van 2005, Wilkinson *et al.* 2005, Chambers *et al.* 2007, Karaoulis *et al.* 2014, Pandey *et al.* 2017). Among them, the direct current resistivity method has been well developed recently which contains information about the types and distributions of subsurface physical properties (Loke *et al.* 2013, Campanella 2008, Oraee *et al.* 2016). When the DC resistivity method applied to coal rock, it measures the potential of electrodes or potential difference between electrodes after supplying electricity into the measured coal rock region to inversely retrieve changes in coal rock apparent resistivity and further effectively determine the internal structure of coal seams. That is, the method diagnoses the geological anomaly area in coalbeds through testing changes in coal rock apparent resistivity (Loke *et al.* 2013, Liu 2014, Wang *et al.* 2016). Because apparent resistivity is highly sensitive to water, it is inevitable that in the hydraulic fracturing process, high pressure water flows along fractured cracks into coal rock mass, leading to changes in apparent resistivity in the coal-rock mass and its

---

∗Corresponding author, Ph.D.
 E-mail: limingloving@cumt.edu.cn

adjacent regions. In general, the region into which high pressure water permeates can be considered as the area effectively affected by hydraulic fracturing. Based on the above, we hypothesize that changes in apparent resistivity in the hydraulic fracturing process could be used to determine the areas impacted by hydraulic fracturing.

To this end, we first analyzed the response principle of coal rock apparent resistivity to hydraulic fracturing using Archie formula. Then we conducted experiments on the apparent resistivity response of small scale coal rock mass to hydraulic fracturing, and analyze the characterstics of apparent resistivity. The results are of significance for exploring new area of coalbed influenced by hydraulic fracturing and ensuring the scientific and safe applications of coal-mine hydraulic fracturing permeability improvement technology.

2. Theoretical analysis of response of coal rock apparent resistivity to hydraulic fracturing

Hydraulic fracturing is a commonly used technology for pressure relief and permeability enhancement in coal mine gas extraction in recent years (Puller *et al.* 2016, Zhou *et al*, 2016). High pressure water is injected into coal seam by drilling, and the coal mass near the borehole is fractured, resulting in the initiation and expansion of the cracks around bole hole, forming a definite range of fracture network and a pressure relief region; thereby increasing the permeability of coal seam, to achieve the effect of efficient gas extraction. Fig. 1 shows the principle effect diagram of hydraulic fracturing.

Archie formula is the empirical relationship between formation resistivity and formation water resistivity, porosity, and water saturation. It was published in 1942 on the law of sandstone resistivity by the United States Shell's oil logging engineer Archie (Hu *et al.* 2017). Combined with the actual conditions of the coal seam, according to Archie formula, the apparent resistivity ρ of the coal seam can be expressed as

$$\rho = \frac{ab\rho_w}{S^n}\phi^{-m} \tag{1}$$

where a and b are two coefficients relevant to coal and rock; ρ_w is the resistivity of high pressure water, ϕ is the porosity of coal rock, S is the saturation; m and n are the cementation factor and the saturation factor of coal rock mass, respectively, which values are more than 1.

The saturation S is the ratio of the volume of water to that of pores and cracks after the intrusion of high pressure water into coal rock mass, and the porosity ϕ is the ratio of pore volume to surface volume.

Hydraulic fracturing technology, on the one hand, can play a good role in pressure relief in the core affect area; on the other hand, it may lead to stress concentration in the adjacent areas. Its influence on the resistivity of coal seams are mainly manifested in two aspects: (1) Directly destroy coal rock mass by high pressure water, changing the porosity of it; (2) High pressure water is quickly injected into coal pores and cracks space before the fracture closed, thus changing the saturation of coal rock mass.
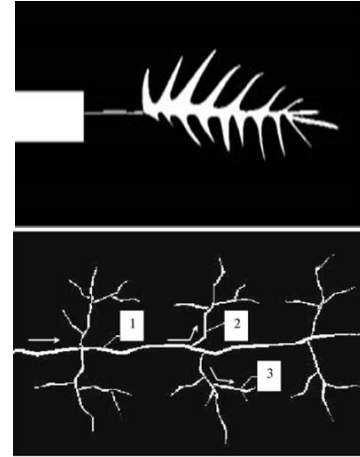

Fig. 1 Schematic diagram of hydraulic fracturing for pressure relief and permeability enhancement. 1, 2, 3 mean first, second and third grade cracks

1) Porosity of coal rock subject to hydraulic fracturing

Coal rock mass can be loaded by hydraulic fracturing with high pressure water. In any loading state, the change in coal porosity is caused by the closure and expansion of microcracks. Thus, the coal rock porosity can be expressed as

$$\phi = \frac{V_0 + \Delta V^c + \Delta V^f}{V} \tag{2}$$

where V_0 is the initial volume of pores of coal rock mass, ΔV^c and ΔV^f is the volume of closed and newly generated pores and cracks, respectively .

From Eq. (2), the relationship of coal rock porosity to the volume strains of pores and cracks in coal seam loading process can be obtained

$$\phi = \phi_0 + \varepsilon_V^c + \varepsilon_V^f \tag{3}$$

where ϕ_0 is the initial porosity; ε_V^c is the closed volume strains of microcracks; ε_V^f is the opened and expanded volume strains of microcracks; wherein $\varepsilon_V^c = \varepsilon_1^c + 2\varepsilon_2^c$ and $\varepsilon_V^f = \varepsilon_1^f + 2\varepsilon_2^f$, ε_1 and ε_2 are the axial and transverse strains, respectively.

2) Porosity of coal rock in the hydraulic fracturing pressure relief zone

After the coal rock mass is pressed down by high pressure water, this area is to convert into a pressure relief zone. A change in coal rock porosity there is caused by the positive slips of closed and expanded cracks in pores and cracks, thus the coal rock porosity can be expressed as

$$\phi = \frac{V_m + \Delta V_a^c + \Delta V_a^f}{V} \tag{4}$$

Eq. (4) can be transformed into the relationship of porosity of pressure relief zone to the volume strain as follows

$$\phi = \phi_m + \varepsilon_a^c + \varepsilon_a^f \tag{5}$$

where ϕ_m is the coal rock porosity corresponding to the pressure relief starting point, ε_a^c and ε_a^f are the closure volume strains of pores and cracks and the positive slip volume strains of the expanded cracks, respectively; and

$$\varepsilon_a^c = \Delta\varepsilon_1^c + 2\Delta\varepsilon_2^c, \ \varepsilon_a^f = \Delta\varepsilon_1^f + 2\Delta\varepsilon_2^f.$$

3) Porosity of coal rock in the stress concentration zone

Hydraulic fracturing can exert an enormous function on the pressure relief and permeability enhancement in the core affected area, but it may lead to the stress concentration in the adjacent area, resulting in stress concentration zone.

After hydraulic fracturing, a change in coal rock porosity in the stress concentration zone depends upon the closure volume of pores and cracks and the positive slip volume of expanded cracks. The coal rock porosity can be obtained by the formula

$$\phi = \frac{V_m + \Delta V_b^c + \Delta V_b^f}{V} = \phi_m + \varepsilon_b^c + \varepsilon_b^f \tag{6}$$

where ϕ_m is coal rock porosity corresponding to the pressure-relief starting point; ε_a^c and ε_a^f are the closure volume strain of pore and cracks and the positive slip volumes strain of the expanded cracks, respectively; and $\varepsilon_b^c = \Delta\varepsilon_1^c + 2\Delta\varepsilon_2^c$ and $\varepsilon_b^f = \Delta\varepsilon_1^f + 2\Delta\varepsilon_2^f$.

Coal rock is a kind of conductor or semiconductor. According to different conductive properties, coal rock can be divided into two sorts: electronic conductivity and ion conductivity. The former is dependent on the free electron conductivity of the basic constituent components of coal rock, while the later is ionically conductive depending on the aqueous solution in pores and cracks. In general, coal rock is electronic conductive materials.

In the hydraulic fracturing process, there will be a large amount of liquid retained in pores and cracks in the area where high-pressure water flows through. Coal rock mass in this area change into mainly ion conductivity, where the porosity and apparent resistivity of the coal rock mass increase.

According to the analysis above, the more residual water in coal, the higher the coal saturation S, the lower the apparent resistivity of the corresponding region; while the resistivity decreases with the porosity increases. The apparent resistivity is inversely proportional to porosity and saturation.

3. Characteristics of response of coal rock apparent resistivity to hydraulic fracturing

3.1 Measurement principle

The DC resistivity testing is a geophysical detecting method based on the difference in electricity conductivity of coal rock mass (Liu *et al.* 2014). It utilizes the spatiotemporal distribution laws of an artificially constructed electrical field to detect the apparent resistivity of coal rock. In the measurement, the supply current with intensity I is input through two embedded current electrodes

A and B into the detected coal rock region and the potential difference ΔU generated at the receiving electrodes M and N by the input current I in the media is measured. Then the apparent resistivity of this region is calculated according to Eq. (7)

$$\rho_s = k\frac{\Delta U}{I} \tag{7}$$

where ρ_s is the apparent resistivity of the medium in the detection region, $\Omega\cdot$m; I is the supply current, A; ΔU is the potential difference, V; k is the coefficient of the electrode system, m, whose value is related to the positions of A, B, M and N. When their positions are fixed, k is a constant can be calculated by Eq. (8)

$$K = \frac{2\pi}{\frac{1}{\overline{AM}} - \frac{1}{\overline{BM}} - \frac{1}{\overline{AN}} + \frac{1}{\overline{BN}}} \tag{8}$$

Using the artificially constructed electric field for resistivity detection is one of the most important electrical detection methods. Its basic measurement principle can be described as follows. The power-supply electrodes of a DC power source, A and B, are embedded in the detection region to form an electric field in the detection region. This electric field distributes differently depending on different media in the detection region such as coal rock, soil, water, etc. If the medium is unitary and uniform, the artificial electric field shows itself as a uniform hemispherical shape. However, affected by its tectonic structure, the medium in the detection region often has high and low resistant ore bodies with different conductivity. When the electric field encounters high resistance ore bodies, the repulsive phenomenon occurs. On the contrary, when the electric field encounters low resistant bodies, the attractive phenomenon appears. Thus, the electric field will changes from a uniform semispheric distribution to inhomogeneous distribution, as shown in Fig. 2. The cloud maps retrieved from the DC resistivity testing experiment could reflect the inhomogeneous distribution of the electric field in the detection area. Thus, analyzing the inhomogeneous electric field distribution can determine the structure and occurrence of geological bodies of different conductivity in the detection area.
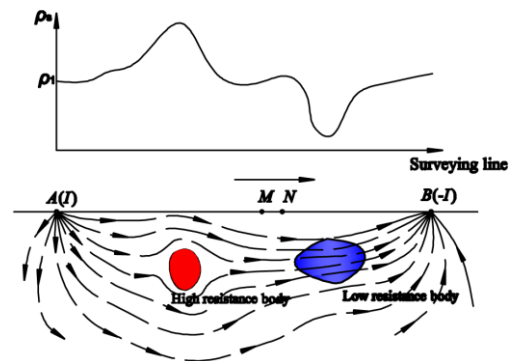

Fig. 2 Schematic of the principle using DC method to detect apparent resistivity
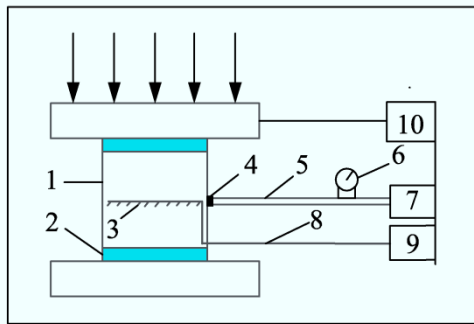
Fig. 3 Schematic of the experimental system. 1-sample, 2-insulation pads, 3-electrode, 4-sealant, 5-water-conducting pipe, 6-pressure gauge, 7-water pump, 8-wires bunch, 9-DC electric measuring instrument and 10-loading press

Fig. 4 WBD-type network parallel electrical instrument

Coal rock is heterogeneous material, containing various defects, including microcracks, pores and joints etc., which are distributed randomly. During the hydraulic fracturing process, the combined action of high pressure water and external stress leads to the instability of different scale defects. Simultaneously, the water will be filled into the poles and cracks in coal rock mass, resulting in reduced apparent resistivity, and the coal rock mass becomes moist and low resistance. At this time, if an external uniform electric field is applied, hydraulic fracturing area will produce a "low resistance to the electric field" (Chen 2012), as shown in Fig. 2, resulting in changes in the apparent resistivity of coal rock mass.

Through the above analysis, it is feasible to analyze the variation of the surrounding electric field and evaluate the affect area of hydraulic fracturing by testing the apparent resistivity.

3.2 Experiments

3.2.1 Experiment system

The experimental system included the loading system, hydraulic fracturing system, and DC resistivity method testing system, as shown in Fig. 3. The loading system was a YAW-type electro-hydraulic servo pressure testing machine consisting of the press machine, automatic load control system and Power Test V 3.3 control program. The hydraulic fracturing system was consisted of high pressure water-conducting pipe, high pressure water meter, and water pump. The data acquisition system was consisted of electrodes, enamel covered copper wire, and WBD-type network parallel electrical instrument (Fig. 4).

Among them, the WBD type network parallel electrical

instrument was mainly consisted of the measurement host, computer and power modules with self-made multi-channel electrode measuring wires. Its main technical specifications are as follows: (1) Number of channels: 16, 48, 64 and 128; 16 channels were used in the experiments. (2) Voltage measuring range:± 10 V, with measured voltage and current accuracy is 0.5% (Full). (3) Maximum emission voltage:15 V / 30 V / 60 V / 90 V. (4) Maximum emission current: 100 mA / 1 A / 2 A. (5) Input impedance> 20 MΩ. (6) Power supply square wave: multi-frequency positive or negative square waves. (7) Operating voltage: 12-18 V with current is 1 A (related to the number of channels).

3.2.2 Sample preparation

Because large-size, regular coal samples were difficult to obtain, according to the actual strength of common coal rock mass, the samples were prepared by mixing the coal powder, gypsum, and cement with their mass ratio of 3:1:1, which uniaxial compressive strength was about 35 MPa, and pouring into size of 150 mm×150 mm×150 mm. After naturally dry for 15 days, a 100 mm deep hole was drilled using a hand driller at the center position of the selected side.

3.2.3 Experimental scheme

In the experiments, first, the axial stress of different value was supplied by the loading system on the sample, then water injection and hydraulic fracturing were implemented on the sample, the apparent resistivity signals were acquired 3 times with 1-hour interval which meant that the date was collected before, during and after each fracturing processes separately. The specific procedure is as follows:

1) Insert one end of the water-conducting pipe into the hole at a 50 mm depth, then use the sealant to seal the hole at the insertion depth, meaning the sealed depth is 50 mm;

2) Attach the electrodes using conductive adhesive to the adjacent side of the sample with a "cross" distribution at the center of the plane, as shown in Fig. 3. All electrodes was spaced in 15 mm and connected with an enamel covered copper wire each;

3) Put the sample on the press machine, connect the enamel covered copper wire with the electric measurement instrument and connect the water-conducting pipe, the water gauge and the water pump together;

4) Vertical loads of 0 kN, 10 kN and 20 kN are supplied by the press machine, the hydraulic fracturing test will be done for each loading stage;

5) After the loading procedure, collect the resistivity date for the first time;

6) Switch on the water pump, inject the high pressure water into the sample through the water-conducting pipe for the hydraulic fracturing, the range of pump pressure in the fracturing process is in 0-10 MPa, and the hydraulic loading rate is 0.05 MPa/s. Observe the crack evolution and the liquid exudation on the sample surface. When lots of water oozes from the sample, turn off the pump and collect the date for the second time;

7) The third date acquisition should be done after the pump shut for 1 hour;

8) Repeat the test three times to ensure the accuracy

under each load;

9) Data analysis and processing.

According to the operational principle of WBD-type network parallel electrical measurement instrument, the monitoring region of the apparent resistivity in experiments is shown in Fig. 5.
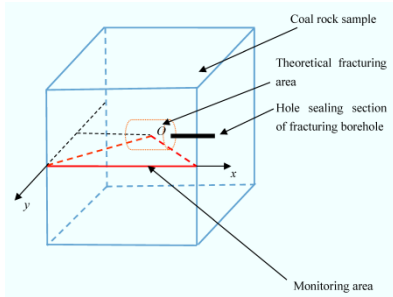

Fig. 5 Monitoring area of WBD-type network parallel electrical measurement instrument as an isosceles right-angled triangle or trapezoid formed by the line connecting electrode with sample gravity center
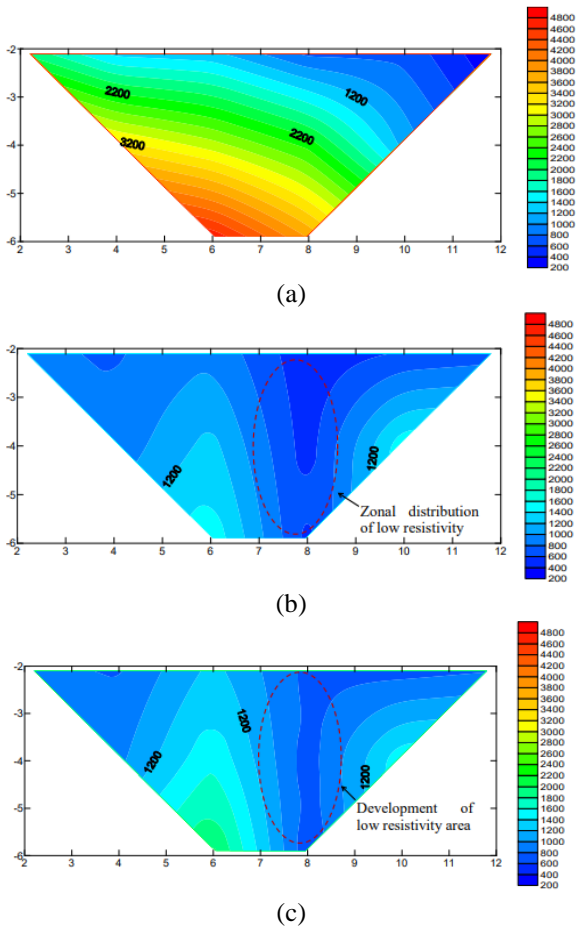

(a)

(b)

(c)

Fig. 6 Cloud maps of apparent resistivity of coal rock samples responding to hydraulic fracturing under external and non-axial loading. (a) Before hydraulic fracturing, (b) Right after hydraulic fracturing and (c) One hour after hydraulic fracturing. The coordinates of cloud maps correspond to Fig. 5, the unit of the apparent resistivity band is Ω•m, and both the units of X and Y-axis are cm. The same below
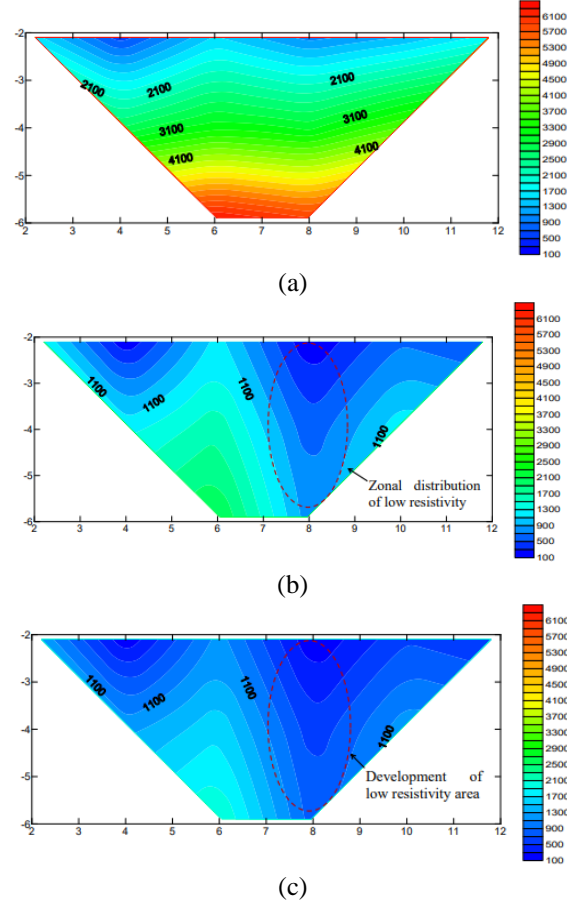

(a)

(b)

(c)

Fig. 7 Cloud maps of apparent resistivity of coal rock samples responding to hydraulic fracturing under external axial load of 10 kN. (a) Before hydraulic fracturing, (b) Right after hydraulic fracturing and (c) One hour after hydraulic fracturing
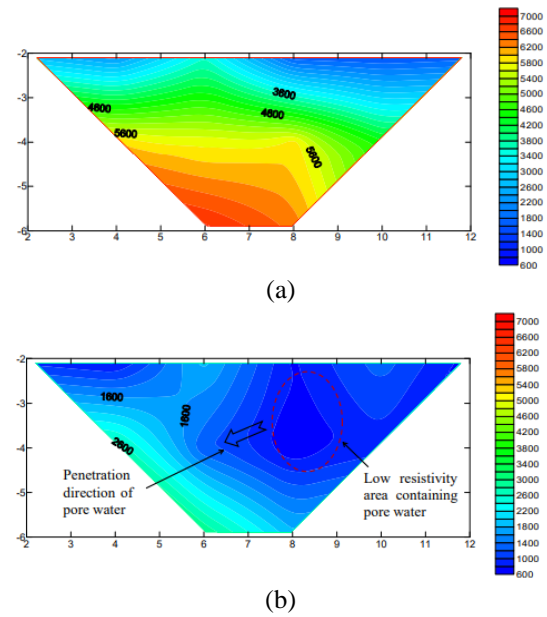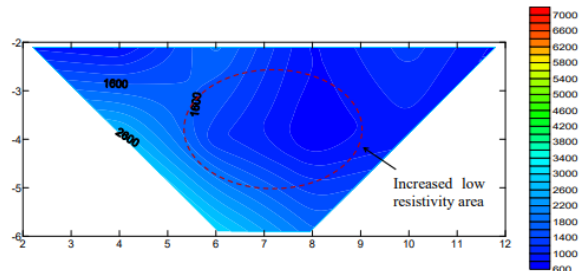

(a)

(b)

Fig. 8 Cloud maps of apparent resistivity of coal rock samples responding to hydraulic fracturing under external axial load of 20 kN. (a) Before hydraulic fracturing, (b) Right after hydraulic fracturing and (c) One hour after hydraulic fracturing

(c)

Fig. 8 Continued

Table 1 Positions of 5 selected points in the apparent resistivity sectional cloud map

axis	Coordinate points				
	A	B	C	D	E
X (cm)	4	5.5	7	8.5	10
Y (cm)	-3	-3	-3	-3	-3

4. Results and analysis

4.1 Cloud maps of apparent resistivity

Figs. 6-8 show typical apparent resistivity cloud maps of coal rock samples at 0, 10 and 20 kN external axial stress in the hydraulic fracturing process.

It can be seen from Figs. 6-8 (a) that the apparent resistivity increases with the increase of axial pressure before fracturing, and the apparent resistivity peak in the middle of the samples at 0 kN, 10 kN and 20 kN is about 4500 Ω•m, 5500 Ω•m, 6500 Ω•m, respectively. After hydraulic fracturing, the apparent resistivity of each sample is reduced. The value of just after hydraulic fracturing is significantly lower than that before fracturing, with a decrease of more than 50%. Contrast with Figs. 6-8 (b), the apparent resistivity inside each sample is not evenly reduced, showing different levels of different regions, some high, some low, and some even appear banding phenomenon.

Compared with Figs. 6-8 (c), the apparent resistivity morphology of each sample after 1 h hydraulic fracturing is similar to that of fracturing just finished. Changes of apparent resistivity of different axial stress samples during the fracturing process are different. When the axial stress is zero, the apparent resistivity decreases first and then increases, and the value of partial area increases after 1 h; while the apparent resistivity of other two samples decreases continuously, that is, $\rho_{\text{before fracturing}} > \rho_{\text{right after fracturing}} > \rho_{\text{1h after fracturing}}$.

4.2 Variations of apparent resistivity at feature points

To further study variation characteristics of coal rock apparent resistivity in the hydraulic fracturing process, 5 points A, B, C, D and E with the same depth and different abscissas were selected in the sectional cloud map. Table 1 shows their positions.

From Fig. 9, it is obvious that the initial apparent resistivity of coal rock samples shows a uneven spatial
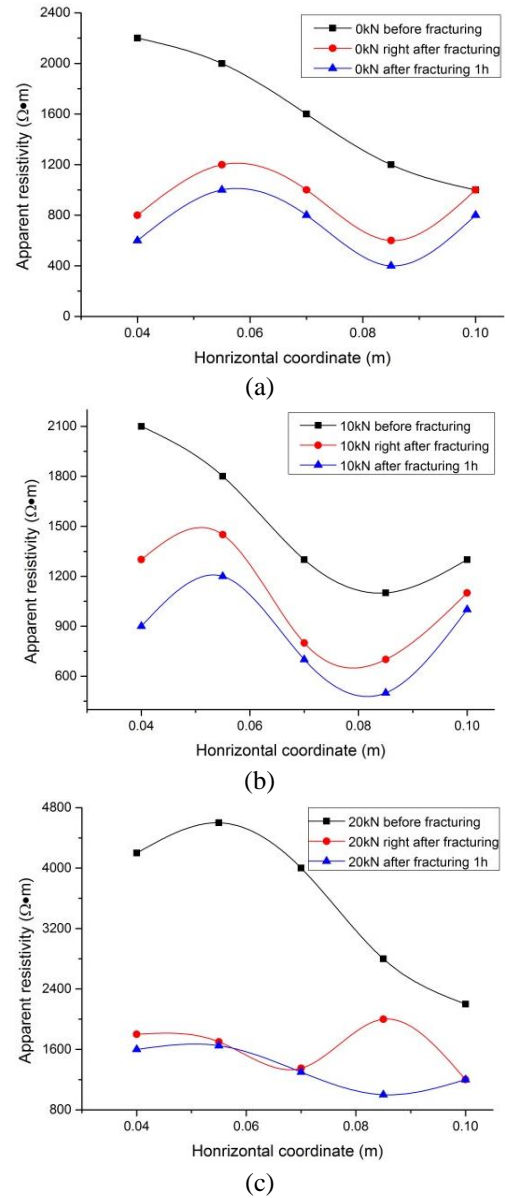

(a)

(b)

(c)

Fig. 9 Relationships of apparent resistivity of coal rock samples to time, space and external load

distribution. It can be deduced by Archie formula that the initial porosity of the samples is also unevenly distributed in space.

Contrast between Figs. 9(b), 9(c) and 9(a) can be further confirmed that with and without external loads, the apparent resistivity of the samples at 1h after and right after hydraulic fracturing have opposite changing trends. In the absence of external loads, the apparent resistivity decreases first and then increases after fracturing; while samples with externally applied loads have a slight decrease in apparent resistivity at 1h after fracturing compared to that right after fracturing.

In addition, we found that although the size of the samples used in this experiment is not large, but variations of the apparent resistivity at different points are not synchronized. On the one hand it shows the heterogeneity of coal rock materials, on the other hand also reflects the high accuracy of our equipments.

4.3 Analysis

Before the fracturing of water injection, different axial loads have already applied to the samples, resulting in different degrees of damage within the samples, and the new generation of numerous pores and cracks, so that the porosity of the sample changed. Since water injection has not yet begun, there was no conductive liquid inside the sample, that is, the saturation did not change. Therefore, the apparent resistivity of the sample was mainly affected by porosity. With the increase of axial load, the porosity of the samples became larger, and the apparent resistivity increased. After water injection, high pressure water on the one hand further damaged the sample structures, increasing the porosity of the sample, on the other hand, it also made water immerse into the pores and cracks and improved the sample water saturation. Water is prone to electric conduction, which changed the initial electric field of coal rocks, and lead to mainly ion conduction of the samples. The apparent resistivity in the area high pressure water flowed through was generally reduced, which is consistent with the description of Archie formula.

Samples in our experiment were made of pulverized coal, gypsum and cement, which cannot be completely homogenized during stirring, resulting in different electrical parameters and strength in different areas. Under the external axial load, some areas due to the small intensity produced a large number of micro-ruptures, while some other areas may maintain a better structure because of the larger intensity. In this way, according to the minimum energy principle (Zhao *et al*. 2003), high pressure water first damaged the area with smaller intensity and then filled cracks, next, cracks were connected to the outside of samples, and finally water flowed out. During this process, the apparent resistivity of the area where water flowed through was significantly reduced, while the area with water immersion and retention decreased more. The zonal distribution of apparent resistivity appeared in the experiments, probably due to the action of high pressure water, resulting in cracks through whole sample and water flowing out from the crack directly and quickly.

After 1 h hydraulic fracturing, the apparent resistivity of samples applied different axial stress showed different variation characteristics. When the axial loads were 10 kN and 20 kN, samples have been destroyed under external load before hydraulic fracturing, resulting in pores and cracks at different scales. High pressure water will be more easily invaded, improve the porosity and saturation, and continuously reduce the apparent resistivity of the samples.

However, the damage energy only supplied by high pressure water for the sample without axial load, which may only produce large scale cracks. After injection finished, water quickly out flowed, resulting in a small amount of moisture remaining in the internal macrocracks that evaporates after a period of time due to ambient temperature, thus the apparent resistivity increases.

It can be seen from the above, under the coupling of water, cracks and stress, water has a dominant effect on the apparent resistivity of coal rock samples. Cracks are the passage ways of high pressure water. If the cracks are filled with water, the area is obviously low resistivity zone; while if water quickly flow out, the apparent resistivity will increase.

5. Conclusions

1) Porosity and water saturation are the two factors affecting the apparent resistivity of coal rock in the hydraulic fracturing process. The apparent resistivity of coal rock mass in various regions can be found by calculating the two factors in these regions.

2) Water has a dominant effect on the apparent resistivity of coal rock samples. The apparent resistivity in the area where water flows through is reduced more than 50%, which can be considered as core affect region of hydraulic fracturing.

3) Stress indirectly impacts the apparent resistivity by changing porosity. Before hydraulic fracturing, the greater axial load applied, the more serious the rupture in the samples, resulting in the greater apparent resistivity. After fracturing, the coal rock apparent resistivity decrease rapidly.

4) Apparent resistivity testing is a potential regional method to evaluate the influence range of hydraulic fracturing in coal seam.

Acknowledgements

References

Ashoori, S., Abdideh, M. and Yahagh, M. (2015), "Investigation of hydraulic fracturing operation and fracture propagation simulation in reservoir rock", *Geomech. Geoeng*., **10**(3), 203-211.

Campanella, R.G. (2008), "The third James K. Mitchell lecture: Geo-environmental site characterization 1", *Geomech. Geoeng*., **3**(3), 155-165.

Chambers, J.E., Wilkinson, P.B., Weller, A.L., Meldrum, P.I., Ogilvy, R.D. and Caunt, S. (2007), "Mineshaft imaging using surface and crosshole 3D electrical resistivity tomography: A case history from the East Pennine Coalfield, UK", *J. Appl. Geophys*., **62**(4), 324-337.

Chen P. (2012), *Direct Current Electric Method Response of Regional Coal and Gas Outburst Danger and its Application*, China University of Mining and Technology Press, Xuzhou, Jiangsu, China.

Guo, C., Yu, H. and Xing, W. (2013), "The key technology of using DC electrical method to detect water-bearing capability of seam roof", *Safe. Coal Mines*, **44**(8), 69-72.

Hou, B., Chen, M., Wang, Z., Yuan, J. and Liu, M. (2013), "Hydraulic fracture initiation theory for a horizontal well in a coal seam", *Petrol. Sci*., **10**(2), 219-225.

Hu, X., Hu, S., Jin, F. and Huang, S. (2017), *Physics of Petroleum Reservoirs*, Springer.

Huang, B., Li, P., Ma, J. and Chen, S. (2014), "Experimental investigation on the basic law of hydraulic fracturing after water pressure control blasting", *Rock Mech. Rock Eng*., **47**(4), 1321-

1334.

Karaoulis, M., Revil, A. and Mao, D. (2014), "Localization of a coal seam fire using combined self-potential and resistivity data", *J. Coal Geol.*,**128**, 109-118.

Lei, Y. and Wen, B. (2014), "Hydraulic fracturing mechanical mechanism analyses for soft seams considering strain softening character", *Adv. Mater. Res.*, **868**, 319-325.

Li, Q., Lin, B., Zhai, C., Ni, G., Peng, S., Sun C. and Cheng, Y. (2013), "Variable frequency of pulse hydraulic fracturing for improving permeability in coal seam", *J. Min. Sci. Technol.*, **23**(6), 847-853.

Lin, B. (2010), *The Theory and Technology of Mine Gas Prevention and Control (Second Edition)*, China University of Mining and Technology Press, Xuzhou, Jiangsu, China, 253-256.

Liu, S., Liu, J. and Yue, J. (2014), "Development status and key problems of Chinese mining geophysical technology", *J. Chin. Coal Soc.*, **39**(1), 19-25.

Loke, M.H., Chambers, J.E., Rucker, D.F., Kuras, O. and Wilkinson, P.B. (2013), "Recent developments in the direct-current geoelectrical imaging method", *J. Appl. Geophys.*, **95**, 135-156.

Oraee, K., Oraee, N., Goodarzi, A. and Khajehpour, P. (2016), "Effect of discontinuities characteristics on coal mine stability and sustainability: A rock fall prediction approach", *J. Min. Sci. Technol.*, **26**(1), 65-70.

Pandey, V.J., Flottmann, T. and Zwarich, N.R. (2017). "Applications of geomechanics to hydraulic fracturing: Case studies from coal stimulations", *SPE Prod. Oper.*, **32**(4).

Puller, J.W., Mills, K.W., Jeffrey, R.G. and Walker, R.J. (2016), "In-situ stress measurements and stress change monitoring to monitor overburden caving behaviour and hydraulic fracture pre-conditioning" *J. Min. Sci. Technol.*, **26**(1), 103-110.

Tu, J., Sun, J., Jiang, Z., Xue, L. and Qian, H. (2013), "Analysis on rock resistivity variation with stress ratio at the state of critial brittle failure", *J. Chin. Coal Soc.*, **38**(2), 221-225..

Van Schoor, M. (2005), "The application of in-mine electrical resistance tomography (ERT) for mapping potholes and other disruptive features ahead of mining", *J. South African Inst. Min. Metal.*, **105**(6), 447-451.

Wang, F., Tu, S., Zhang, C., Zhang, Y. and Bai, Q. (2016), "Evolution mechanism of water-flowing zones and control technology for longwall mining in shallow coal seams beneath gully topography", *Environ. Earth Sci.*, **75**(19), 1309.

Wilkinson, P.B., Chambers, J.E., Meldrum, P.I., Ogilvy, R.D., Mellor, C.J. and Caunt, S. (2005), "A comparison of self-potential tomography with electrical resistivity tomography for the detection of abandoned mineshafts", *J. Environ. Eng. Geophys.*, **10**(4), 381-389.

Yan, Z., Ju, Y., Tang, S., Hou, Q., Zhu, B. and Wang, G. (2013), "Numerical simulation study of fracturing process in coalbed methane reservoirs in southern Qinshui basin", *Chin. J. Geophys.*, **56**(5), 1734-1744.

Zhang, J. (2014), "Numerical simulation of hydraulic fracturing coalbed methane reservoir", *Fuel*, **136**, 57-61.

Zhao, Y., Feng, Z. and Wan, Z. (2003), "Least energy principle of dynamical failure of rock mass", *Chin. J. Rock Mech. Eng.*, **22**(11), 1781-1783.

Zhou, F., Xia, T., Wang, X., Zhang, Y., Sun, Y. and Liu, J. (2016). "Recent developments in coal mine methane extraction and utilization in China: A review", *J. Nat. Gas Sci. Eng.*, **31**, 437-458.

Zhou, G., Yu, Y. and Cheng, W. (2013), "Simulation experimental study on the permeability of coal rock in deep mine", *Proceedings of the 3rd International Conference on Applied Mechanics, Materials and Manufacturing (ICAMMM 2013)*, Dalian, China, August.

Zhu, K., Guo, D., Zeng, X., Li, S. and Liu, C. (2014), "Proppant flowback control in coal bed methane wells: Experimental study and field application", *J. Oil Gas Coal Technol.*, **7**(2), 189-202.

CC